

# Aliasing of unmodeled gravity effects in estimates of non-conservative force coefficients

Vishal Ray\* and Daniel J. Scheeres†  
University of Colorado Boulder, Boulder, CO 80309-0020

In most satellite tracking operations, the gravity field is truncated at an order and degree based on their average effects on the motion of the satellite. Even though the contribution of the higher degree/order gravitational harmonics towards the propagation of the satellite states may be negligible as seen in isolation from other forces, their aliasing with the non-gravitational force coefficients can significantly affect the prediction capabilities in the tracking process. The correlation of the gravity field with the non-gravitational forces of atmospheric drag and solar radiation pressure (SRP) renders the estimates of their force coefficients non-physical which in turn degrades the accuracy of the predicted satellite states. This occurs since the magnitude of instantaneous higher-order gravity field acceleration can be as large as the non-gravitational accelerations up to degree and order 140 at around 350 km altitude, even though their net effect is averaged out for long-term motion. Therefore, an arbitrary order of truncation of the gravitational field model is detrimental to orbit determination. It is imperative to select the order depending on the altitude and factors such as area-to-mass ratio that affect the non-conservative forces. In this work, we study the correlations between these forces across varying orbit altitudes. The order and degree to which the gravitational field should be modeled in order to mitigate the effects of the correlation with the non-gravitational force coefficients is derived for different orbital regimes. The sensitivity of the aliasing effects on the coefficients to factors that govern the magnitude of the non-conservative forces relative to the gravitational force is investigated. We show that the error introduced in the coefficients due to the aliasing effects can be predicted based on the ratio of the gravitational force projected along the direction of the non-conservative force. Finally, error maps for the coefficient estimates are presented to aid the selection of truncation error at various altitudes in the low altitude LEO regime.

## I. INTRODUCTION

### A. Purpose of study

THE estimation of non-conservative force coefficients during orbit determination has been a long standing problem in the field of space situational awareness. Obtaining accurate estimates of these parameters is important not only for long-term orbit prediction but also for scientific applications such as derivation of atmospheric densities from drag acceleration. The most dominant non-conservative forces in the low Earth orbit (LEO) regime are atmospheric drag and solar radiation pressure (SRP). The drag acceleration is given by

$$\mathbf{a}_{drag} = -\frac{1}{2}\rho C_d \frac{A_{ref}}{m} v_r^2 \hat{\mathbf{u}} \quad (1)$$

where  $\rho$  is the atmospheric density,  $C_d$  is the drag coefficient,  $v_r$  is the relative velocity of the satellite w.r.t the atmosphere,  $\hat{\mathbf{u}}$  is the unit vector in the relative velocity direction,  $m$  is the mass of the satellite and  $A_{ref}$  is the reference cross-sectional area. The SRP acceleration is given by

$$\mathbf{a}_{SRP} = P_s \frac{C_r}{m} A \frac{\mathbf{r}_s}{|\mathbf{r}_s|^3} AU^2 f_s \quad (2)$$

where  $P_s$  denotes the solar radiation pressure equal to 4.56  $\mu\text{Pa}$  at 1 AU distance,  $C_r$  is the radiation drag coefficient,  $A$  is the cross-sectional area along the sun direction,  $\mathbf{r}_s$  is the position vector w.r.t the sun in inertial frame, AU denotes 1 Astronomical Unit and  $f_s$  denotes the shadow function. In many orbit determination applications, the drag coefficient ( $C_d$ ) that governs gas-surface interactions and SRP coefficient ( $C_r$ ) that governs photon-surface interactions in orbit are

\*PhD Student, Aerospace Engineering and Sciences, Boulder, Colorado, vira0155@colorado.edu

†Distinguished Professor, Aerospace Engineering and Sciences, Boulder, Colorado, scheeres@colorado.edu

estimated as constants, commonly known as the cannonball model [1]. Since these interactions vary throughout the orbit, the coefficients are dependent on various time-varying parameters and are not constant. Therefore, assuming a constant model for them degrades the accuracy of orbit determination (OD) and orbit prediction (OP) and introduces biases in applications such as atmospheric density estimation. The errors in the estimates of these coefficients obtained during OD have been attributed to the assumption of a constant value; therefore, various high-fidelity models have been proposed to capture the variation of these coefficients and improve the accuracy of their estimates [2–6]. If all other modeling errors have been accounted for, such high-fidelity models can be beneficial for OD and OP. But estimation of free parameters in a filtering methodology is plagued by the issue of aliasing with other unmodeled errors. Therefore, even with high-fidelity models of these coefficients, the estimates will still be inaccurate if there are other unmodeled effects in the filter. Even though an apparently ‘good’ orbit fit may be obtained in such a case, the prediction accuracy will degrade rapidly. Prime examples are error in atmospheric density that gets directly absorbed in the drag coefficient estimate and shadow mismodeling for the SRP coefficient. Other modeling errors include tidal forces, thermal radiation pressure, etc. The accuracy degradation of non-conservative force coefficient estimates is dependent on the relative magnitude of the component of unmodeled forces along the direction of the non-conservative force. For example, an unmodeled force with a larger component along SRP direction than drag will introduce a larger error in the SRP coefficient than the drag coefficient.

We would like to bring to attention the corrupting effects that arbitrary truncation of the gravity field can have on estimates of the drag and SRP coefficients in the LEO regime. The geopotential is given by [7]

$$U = \frac{GM_e}{r} \sum_{n=0}^{\infty} \sum_{m=0}^n \frac{R_e^n}{r^n} P_{nm}(\sin \phi)(C_{nm} \cos(m\lambda) + S_{nm} \sin(m\lambda)) \quad (3)$$

where  $G$  is the universal gravitation constant,  $M_e$  is the mass of Earth,  $R_e$  is Earth’s radius,  $r$  is the distance from Earth’s center,  $\phi$  and  $\lambda$  are the geocentric latitude and longitude respectively,  $P_{nm}$  are Legendre polynomials of degree  $n$  and order  $m$ , and  $C_{nm}$  and  $S_{nm}$  are coefficients that describe the dependence of the potential on Earth’s internal mass distribution. The geopotential is truncated at a degree  $n$  and order  $m$  in OD models for computational reasons. The order and degree of truncation has generally been based on the diminishing contribution of higher order terms towards orbit propagation [8, 9]. Even though the averaged effects of the higher degree/order geopotential terms on the orbit propagation are comparatively small, the instantaneous acceleration due to these terms can be higher than the dominant drag and SRP forces to a significantly larger degree and order. As a result, the ignored gravitational acceleration aliases into the estimated drag and SRP coefficients. Consequently, the effective contribution of the unmodeled geopotential to orbit prediction accuracy is much larger than anticipated purely due to propagation. Therefore, the suggested truncation orders of the geopotential [8–10] for OD and OP in LEO do not hold when the drag and SRP coefficients are being estimated. The correlation of the truncated geopotential with the drag and SRP coefficient has been hinted at [9, 11] but we couldn’t find any comprehensive study mapping out these correlations across LEO altitudes. As pointed out by the National Academy of Engineering (NAE) [11], “*in the current orbit determination process, any errors caused by the omission of high-degree and high-order gravity terms will be non-physically absorbed into terms such as the ballistic coefficient, even though they minimize the residuals and result in state estimations that are satisfactory to current requirements.*” The same study also points out that the current special perturbations (SP) catalog, i.e. the catalog maintained by using full numerical integration to generate ephemerides for the satellites, utilizes a medium fidelity (36x36) geopotential. We show that truncation at this order/degree introduces significant errors in the cannonball drag and SRP coefficient estimates that ultimately leads to poor orbit prediction accuracy in LEO altitudes.

## B. Outline

In this work, we analyze the correlations between higher order gravitational forces and the non-conservative forces of SRP and atmospheric drag in the low altitude LEO regime, i.e. 350-850 km. In section II, the simulation setup for the analysis is described. Section III compares the instantaneous and average acceleration magnitudes of the forces. As noted before, it is important to look at both the instantaneous and average accelerations in order to predict the errors introduced in the coefficients due to aliasing. Section IV gives the relative error of the coefficient estimates as a function of the gravity field truncation order/degree. The correlations between the forces will vary as the orbital conditions change. In particular, the gravity field experienced by a satellite in near-polar orbit is different from a near-equatorial orbit because of the dominance of different gravitational harmonics in the two regimes. The magnitude of drag and SRP relative to higher order gravity also depends on factors such as the satellite area-to-mass ratio and solar activity level. Therefore, a sensitivity analysis is carried out to analyze changes in the estimation error trends with these factors. For

orbit propagation, using a non-square gravity potential, i.e. different degree and order, can be beneficial over a square gravity field, i.e. same degree and order [8, 9]. This is because higher order zonal terms ( $m = 0$ ) can have a significantly larger contribution to orbit propagation than higher order tesseral ( $m < n$ ) and sectorial ( $m = n$ ) terms. Section VI analyzes if this holds true when drag and radiation coefficients are being estimated. Finally, estimation errors in the drag and radiation coefficients are mapped out over an altitude range of 350-850 km as a function of gravity field truncation order/degree along with the resulting orbit prediction errors at the end of three days in section VII.

## II. SIMULATION SETUP

This section provides details on the dynamics model, measurements and filtering methodology used in the study. The forces in the true dynamics and filter dynamics models are summarized in Table 1. EGM2008 [12] is used as the gravity model in the simulations. NRLMSISE-00 [13] is used as the atmospheric density model for the drag force. A shadow function models the umbra and penumbra in Eq. 2 [7]. JPL's DE-430 ephemerides are used for the position of Sun and Moon [14].

True dynamics	Filter dynamics
200x200 Geopotential	Truncated geopotential
Cannonball atmospheric drag	Cannonball atmospheric drag, Cd is estimated
Cannonball SRP	Cannonball SRP, Cr is estimated
Third-body forces of Sun and Moon	Third-body forces of Sun and Moon

**Table 1 Forces used in the true and filter dynamics models. EGM2008 is used for the geopotential**

The state vector being estimated in the filter consists of the satellite position, velocity, drag and radiation coefficients. The initial orbital elements are given in Table 2. Orbits in the altitude range of 350-850 km are analyzed. The orbits are assumed to be circular and the variation of the coefficients in orbit is ignored. This allows the analysis of the errors introduced in the coefficients purely due to unmodeled gravity. The area-to-mass ratio of the satellite is taken as 0.04 for both drag and SRP forces.

GPS position and velocity measurements are assumed to be available every 10 s with noise standard deviations of 1.5 m and 0.5 cm/s respectively. A batch filter is used to process a data arc of 1 day and the orbits are then predicted for the next three days. The details of the measurement model and filtering methodology can be found in [15].

Element	Value
e	0
i	90 <sup>0</sup>
$\Omega$	0 <sup>0</sup>
u	0 <sup>0</sup>

**Table 2 Initial orbital elements of the satellite in study**

## III. ACCELERATION ORDER OF MAGNITUDE ANALYSIS

In this section, a comparison of higher order gravity, drag and SRP acceleration magnitudes is presented. The correlations between a truncated gravity field and non-conservative forces exist because of the presence of components of the unmodeled gravity along the direction of the latter. The filter then tries to adjust the free parameters, the drag and radiation coefficients, according to the magnitude of the error in the truncated gravity in velocity and sun directions respectively. In order to compare the acceleration magnitudes, the unmodeled gravitational acceleration is projected

along the relative velocity direction in Eq. 1 and the sun-satellite direction in Eq. 2.

$$g_{drag}(t) = \{\mathbf{g}_{200 \times 200}(t) - \mathbf{g}_{m \times n}(t)\} \cdot \hat{\mathbf{u}}(t) \quad (4)$$

$$g_{SRP}(t) = \{\mathbf{g}_{200 \times 200}(t) - \mathbf{g}_{m \times n}(t)\} \cdot \hat{\mathbf{r}}_s(t) \quad (5)$$

where  $g_{drag}(t)$  is the projection of the unmodeled gravity, i.e. the gravity acceleration error, along the drag direction at time  $t$ ,  $\mathbf{g}_{n \times m}$  is the gravity acceleration truncated at degree  $n$  and order  $m$ ,  $\mathbf{g}_{200 \times 200}$  is assumed to be the true gravity acceleration,  $g_{SRP}(t)$  is the projection of the unmodeled gravity along the sun direction at time  $t$  and,  $\hat{\mathbf{u}}(t)$  and  $\hat{\mathbf{r}}_s(t)$  are the drag and SRP directions defined in Eqs. 1 and 2 at time  $t$ . The instantaneous projected acceleration errors are then averaged over one day, i.e., the length of the estimation data-arc, to obtain the average projected gravity acceleration errors.

$$\bar{g}_{drag} = \frac{1}{T} \int_0^T g_{drag}(t) dt \quad (6)$$

$$\bar{g}_{SRP} = \frac{1}{T} \int_0^T g_{SRP}(t) dt \quad (7)$$

where  $T$  denotes one day. Similarly, the drag and SRP accelerations are averaged over a day. The average acceleration magnitudes are plotted in Fig. 1 at 350 km altitude and 850 km as a function of truncation order/degree. Since the drag and SRP acceleration magnitudes are independent of the gravity truncation, they are represented as constant lines in the figure. The first observation from the figure is that the average gravity acceleration errors projected along the velocity and sun directions do not monotonically decrease with the truncation order/degree. This observation is consistent with Barker et al. [9] that higher order tesserals can have cancelling effects at low truncation degrees in lower altitudes. At 350 km, the average drag is an order of magnitude higher than the gravity acceleration error along the velocity direction for a 10x10 field and the difference in magnitude increases for higher truncation orders. On the other hand, the average SRP is comparable to the average gravity acceleration error along the sun direction and in fact lower in magnitude until degree/order 60. It is expected that the error introduced in the SRP coefficient will be much higher than the error in the drag coefficient at 350 km. At 850 km, both are comparable to the gravity acceleration error at the lower truncation orders and it is expected that similar errors will be introduced in both the estimated coefficients.

Even though the average drag and SRP seem to be larger than the gravity errors after particular truncation orders, the instantaneous gravity acceleration errors are comparable to them until a much higher truncation order. As can be seen in Fig. 2, the instantaneous gravity acceleration errors can be higher than drag up to order 100 at 350 km and up to around order 90 at 850 km. For SRP, gravity acceleration error dominates over SRP for orders even higher than 100 at 350 km.

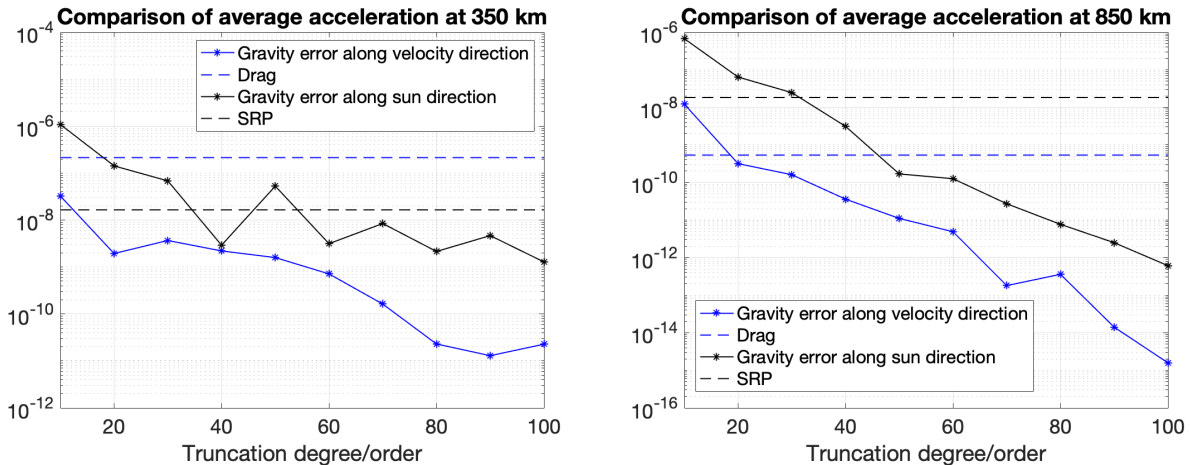


**Fig. 1 Comparison of absolute average gravity acceleration errors with drag and SRP accelerations at 350 km (left) and 850 km (right). Note that the gravity error acceleration curve plots the difference between a 200x200 gravity field and a gravity field truncated at an order/degree specified by the x-axis**

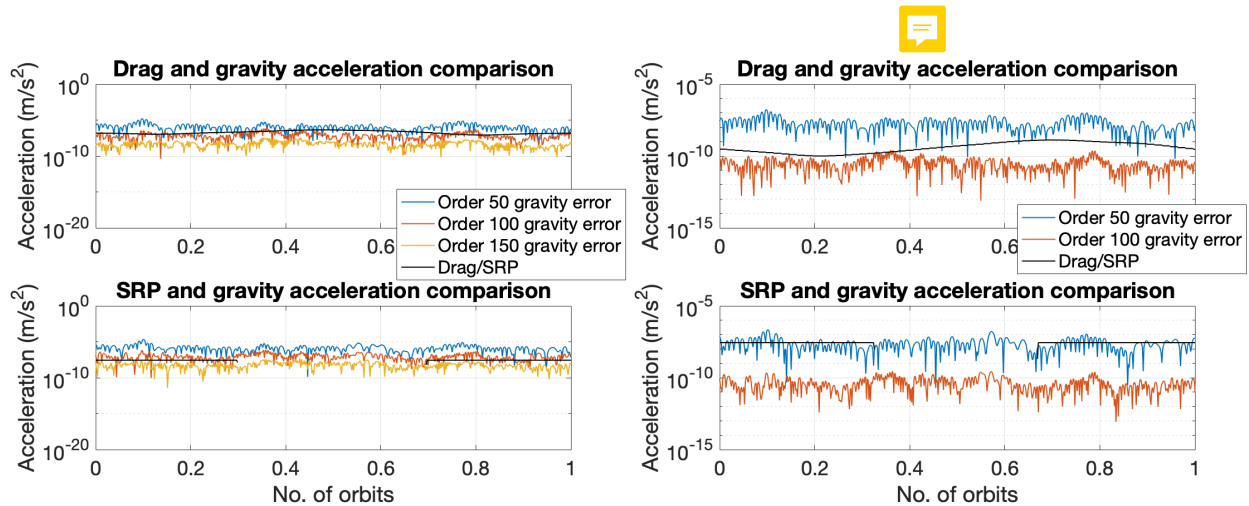


**Fig. 2 Comparison of absolute instantaneous gravity acceleration errors with drag and SRP accelerations at 350 km (left) and 850 km (right). Note that the gravity error acceleration curve plots the difference between a 200x200 gravity field and a gravity field truncated at an order/degree specified by the x-axis**

#### IV. COEFFICIENT ESTIMATES

This section describes the trends of the errors introduced in the coefficient estimates as a function of the gravity field truncation degree/order and the consequence on orbit prediction. The truth and filter dynamics models from section II are used to estimate the satellite states, and the drag and SRP coefficients. The relative error ( $\epsilon$ ) in the coefficients for each gravity truncation order in the filter is defined as follows

$$\epsilon = \frac{|\tilde{C} - C|}{C} \quad (8)$$

where  $C$  is the true value and  $\tilde{C}$  is the estimated value of the coefficient at a particular gravity truncation order in the filter. The relative errors in the coefficient estimates along with the ratio of average projected gravity error and the average drag/SRP acceleration are plotted in Fig. 3. The relative error in the coefficients can be seen to be quite high for low truncation orders. At 350 km, the relative error in SRP coefficient is much higher than in drag coefficient while at 850 km, they are similar at any given truncation order/degree. This follows directly from the discussion in the previous section. Another intuitive observation is that the relative error in the coefficients closely follows the trend of the acceleration ratios. At 850 km, the trends are similar until a certain order/degree and then the coefficient errors plateau out. The maximum accuracy with which the coefficients can be estimated is determined by the contribution of the force towards the orbit propagation. Since the contribution of drag is much higher at 350 km than at 850 km, the drag coefficient can be estimated to a higher relative accuracy given a high truncation order/degree. The SRP coefficient plateaus out to similar relative errors at both the altitudes but at different truncation orders. It is interesting that the SRP coefficient error follows the acceleration ratio trend more closely than the drag coefficient error. This is probably because SRP remains almost constant during short time scales in the orbit while drag changes significantly according to the atmospheric density. Therefore, the average force is an effective measure of the total SRP in orbit but for drag, the average does not capture the net force very well.

From Fig. 3, it apparently seems that the truncation order at 350 km is governed by the SRP coefficient since the relative error is much higher for SRP than drag at any order. But it should be kept in mind that the SRP acceleration is almost an order of magnitude smaller than drag at that altitude as seen in Figs. 1 and 2. Therefore, a small relative error in drag might be more significant for orbit prediction than a large relative error in SRP. The truncation order of the gravity field for OD should be determined by the overall effect of the errors introduced in these coefficients towards orbit propagation. Therefore, a sensitivity analysis is performed to determine the overall effect of a certain relative error on the orbit accuracy. The drag and SRP coefficients are perturbed individually and the orbit is propagated for three days. The position error root-mean-square (RMS) value is then noted down. The analysis is performed for altitudes in the range 350-850 km and the RMS values are plotted w.r.t the altitude in Fig. 4. Note that in the figure when one coefficient is perturbed, the other is kept constant and that the SRP coefficient is perturbed by hundred times higher

relative errors than drag. It can be seen that the effect of relative error in  $C_d$  is higher than  $C_r$  at all altitudes. Even at 850 km, 10 % error in  $C_d$  results in higher orbit error than 10 % error in  $C_r$ . The contribution of  $C_r$  increases slowly with altitude since SRP force does not change significantly in low LEO regime while the contribution of  $C_d$  drops exponentially because of atmospheric density. Figs. 4 and 3 can be used to determine the minimum gravity truncation order at 350 and 850 km. For example, at 350 km, a 0.1 % error in  $C_d$  results in a position error RMS of 10 m at the end of three days. From Fig. 3, it can be seen that in order to reach a 0.1 % , i.e.  $10^{-3}$  relative error, a minimum gravity order of 90 is required. In the same figure, at order 90, the relative error in  $C_r$  is around 0.1, i.e. 10 %. From Fig. 4, a 10 % error in  $C_r$  contributes to less than 1 m position error RMS at the end of three days. It should be noted that the errors in Fig. 4 are purely due to propagation with no other error than the coefficients. In OD, the errors will be much higher since the estimated initial state will have errors and both the coefficients will be perturbed from their true values along with any other modeling errors. Therefore, the figure serves only as a qualitative reference for the relative effects of the drag and SRP coefficient error on the orbit propagation at different altitudes.

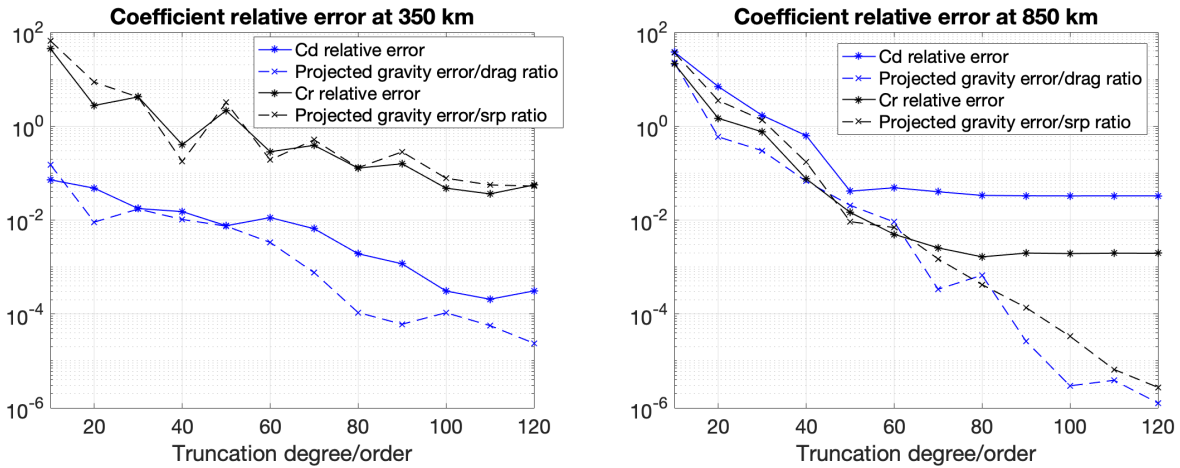


**Fig. 3** Relative errors in the drag and SRP coefficient estimates as a function of the truncation order/degree of the gravity field model in the filter at 350 km (left) and 850 km (right). The ratio of the projected gravity error along the velocity/sun direction and the drag/SRP acceleration is plotted for reference

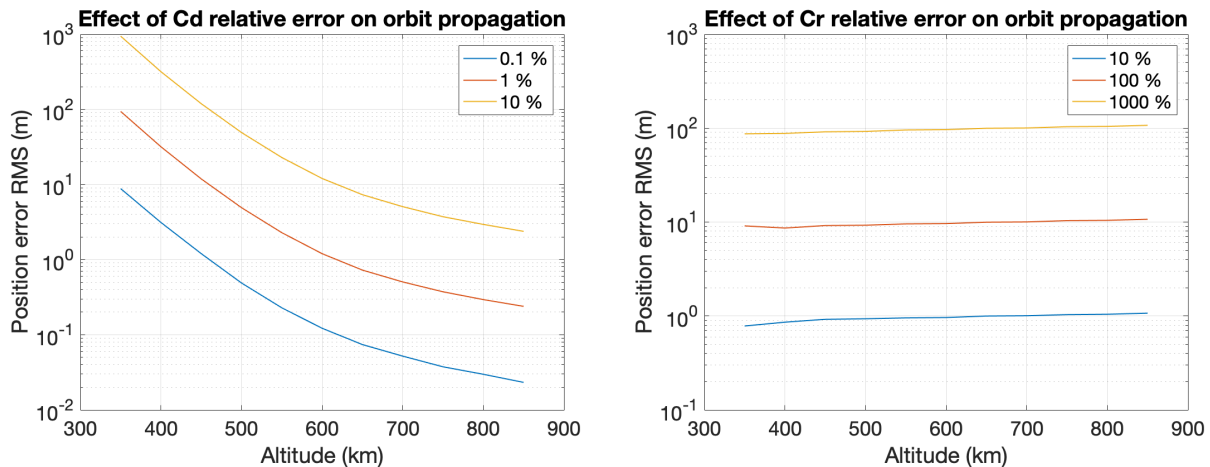


**Fig. 4** The sensitivity of orbit propagation to errors in drag coefficient (left) and SRP coefficient (right)

## V. SENSITIVITY ANALYSIS

In this section, the sensitivity of the coefficient relative errors to several factors is studied. The variation of gravity and the non-conservative forces depends on several factors including orbital elements, solar activity level that changes the state of the atmosphere and area-to-mass ratio that determines the magnitude of the non-conservative forces acting on the satellite. The extent of correlations between the forces can change according to these conditions. Therefore, it is valuable to understand how the trend of estimation error in the coefficients changes with these factors. Specifically, the change in the truncation order/degree to obtain a certain accuracy in the estimated coefficients with these factors needs to be analyzed. In the following discussions, the parameters are changed in both the true and filter dynamics models, i.e., there's no dynamics mismodeling other than gravity.

### A. Orbit inclination

As seen in the previous sections, the correlations are highly dependent on the altitude of the satellite since it changes the relative magnitude of the forces. Since eccentricity changes the altitude of the satellite, the correlations will depend on the orbit eccentricity as well. But since the drag coefficient changes with altitude, a constant cannonball coefficient will not suffice for a highly eccentric orbit. It becomes non-trivial to analyze the aliasing into the drag coefficient estimate in such a case since there's no 'true' cannonball drag coefficient. In this study, we look at the correlations only for a circular orbit. The other orbital element that changes the nature of the forces acting on the satellite, especially gravity, is orbital inclination. Till now, all the analyses have been carried out for a polar orbit. The drag and SRP coefficient estimation errors as a function of gravity truncation degree/order for a near-equatorial orbit with an inclination of  $15^\circ$  and a polar orbit at 350 km are plotted in Fig. 5. The figure also plots the maximum prediction error at the end of the three days, obtained by propagating the initial state estimate forward. The error trends are similar for both the inclinations but the drag coefficient error is smaller for the near-equatorial orbit than the polar orbit. This is because, near the equator, the altitude from the surface is smaller than at the poles for the same semi-major axis. Therefore, the drag force is larger due to the increased density which reduces the aliasing of the unmodeled gravity into the drag coefficient following the discussion from section III. There's a large reduction in the drag coefficient error at truncation degree/order 70 which leads to a reduction in the prediction error. It is safe to say that by order 80, the errors for both the orbits are quite low.

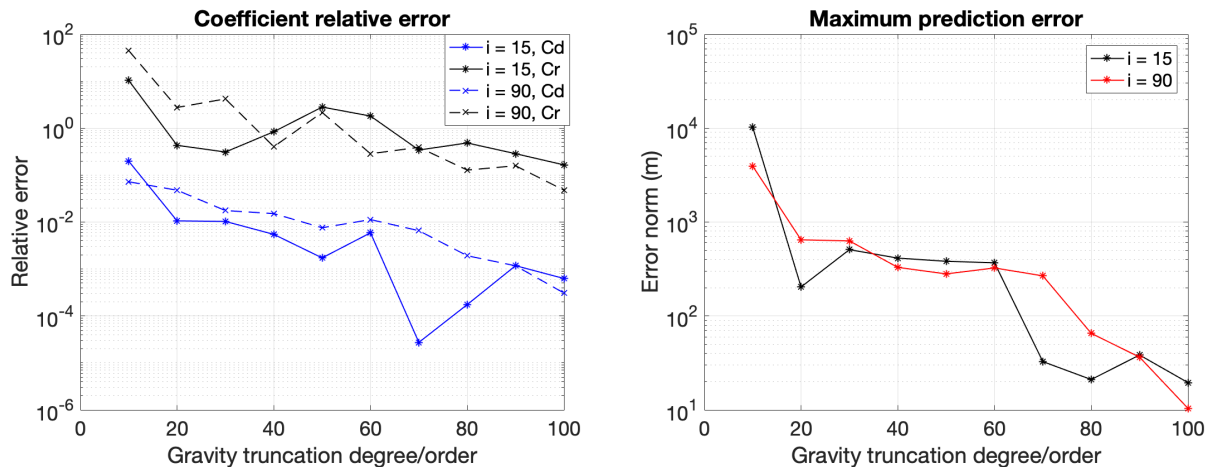
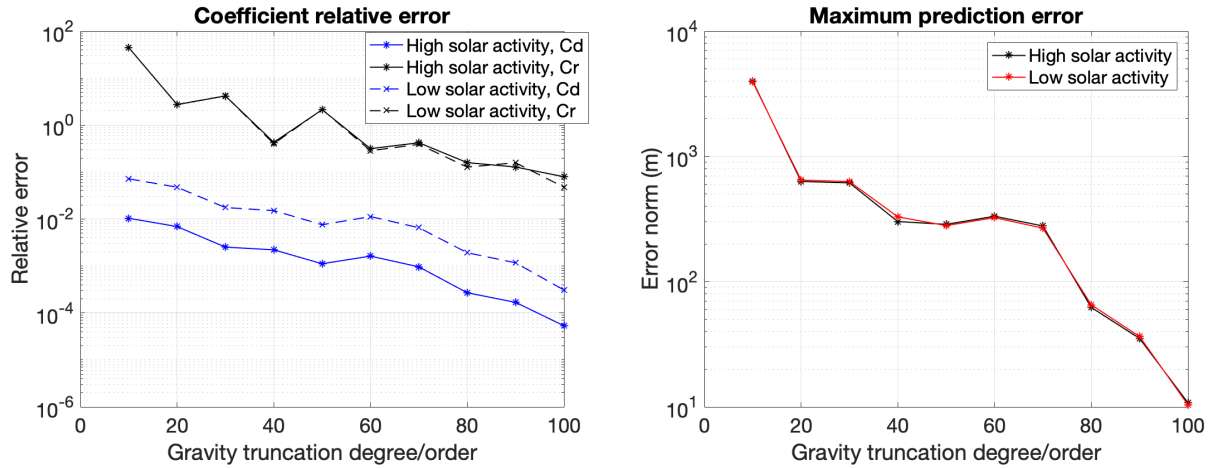


Fig. 5 Relative error in the estimated coefficients (left) and maximum error in the predicted orbits at the end of three days (right) for two orbital inclinations at 350 km

### B. Solar activity level

The atmosphere is highly sensitive to the solar activity level and atmospheric density can change by orders of magnitude with solar activity. During times of high solar activity, expansion of the atmosphere leads to increased density at all altitudes. Therefore, the relative magnitude of drag w.r.t gravity, i.e. the correlation between the forces changes. On the other hand, SRP is relatively unaffected since the change in the total solar irradiance is only 0.1-0.2 % in a solar cycle [16]. The relative errors in the estimated coefficients for a  $F10.7 = 200$  (high solar activity) and  $F10.7 =$

65 (low solar activity) is compared in Fig. 6. As expected, the error in the drag coefficient changes by almost an order of magnitude while the radiation coefficient error remains almost the same. The drag coefficient relative error decreases since the magnitude of the drag force w.r.t the gravity increases. But since the drag force is larger for a higher solar activity, the orbit propagation is more sensitive to errors in the drag coefficient. Therefore, a smaller error in  $C_d$  at any truncation order/degree does not imply a smaller error in the predicted orbit as shown by the right figure in Fig. 6 where the prediction errors remain the same in both the cases.



**Fig. 6** Relative error in the estimated coefficients (left) and maximum error in the predicted orbits at the end of three days (right) at 350 km during high solar activity ( $F_{10.7} = 200$ ) and low solar activity ( $F_{10.7} = 65$ )

### C. Area-to-mass ratio (AMR)

The magnitude of the non-conservative forces acting on the satellite is directly proportional to the AMR in the direction of that force. The estimation errors in the coefficients are plotted for three AMRs in Fig. 7. The figure also shows the maximum prediction errors at the end of three days. The relative error in the coefficients scale inversely with the AMRs since the magnitude of the forces relative to the gravity force increases with increasing AMR. But as seen earlier, even though the relative error is smaller for a higher magnitude force, the sensitivity of the orbit propagation to the coefficient is higher. This can be seen in the position error plot where the error curves are similar for all the AMRs.

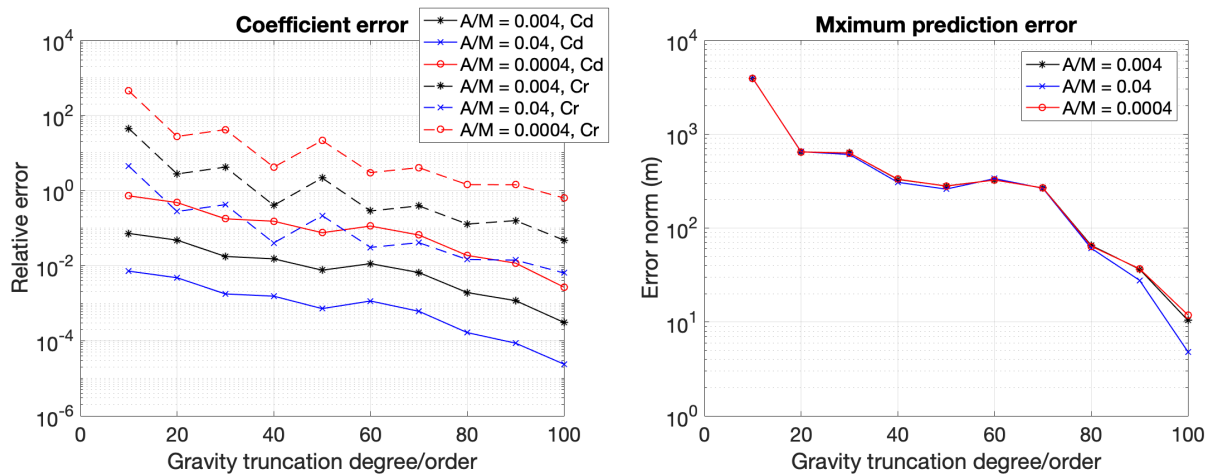


**Fig. 7** Relative error in the estimated coefficients (left) and maximum error in the predicted orbits at the end of three days (right) at 350 km for three satellite area-to-mass ratios



## VI. NON-SQUARE GRAVITY FIELD

In this section, the effects of higher order tesseral terms on the coefficient relative errors are analyzed. It has been pointed out in literature that non-square gravity fields can sometimes be more beneficial for orbit propagation than square gravity fields [8, 9], i.e. higher degree zonal terms have more contribution towards the propagation than higher order tesseral terms. In order to investigate if the same holds true for the aliasing with the drag and SRP coefficients, tesseral terms until order 40 are included and zonal terms are increased from degree 40 to degree 90. Fig. 8 plots the the coefficient relative errors and maximum prediction error as a function of the zonal truncation degree. It can be seen that even though the maximum prediction error keeps decreasing until order 70 and then reaches a steady state, the errors in the coefficients increase slightly. Next, all the zonal terms (i.e. until degree 200) are included and the tesseral terms are truncated in the filter gravity model. The relative errors in the estimated coefficients are plotted in Fig. 9 as a function of the tesseral order truncation. The relative error in the SRP coefficient becomes almost constant after order 50 but the drag coefficient error keeps decreasing. The maximum prediction error also does not seem to reach a steady state and keeps decreasing for higher tesseral orders. Therefore, a non-square field does not seem to be advantageous when drag and SRP coefficients are being estimated.

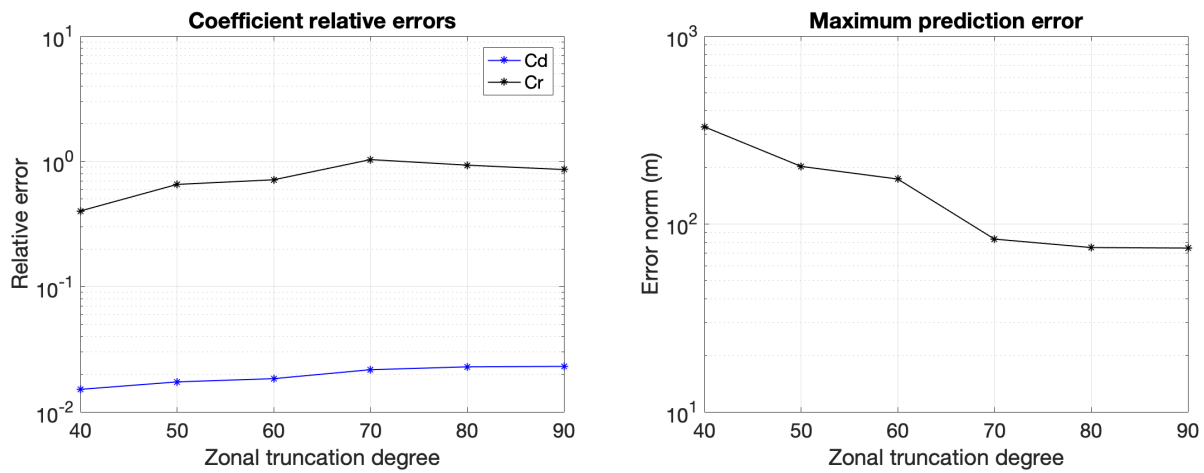


Fig. 8 Relative error in the estimated coefficients (left) and maximum error in the predicted orbits at the end of three days (right) at 350 km with tesseral terms fixed at order 40

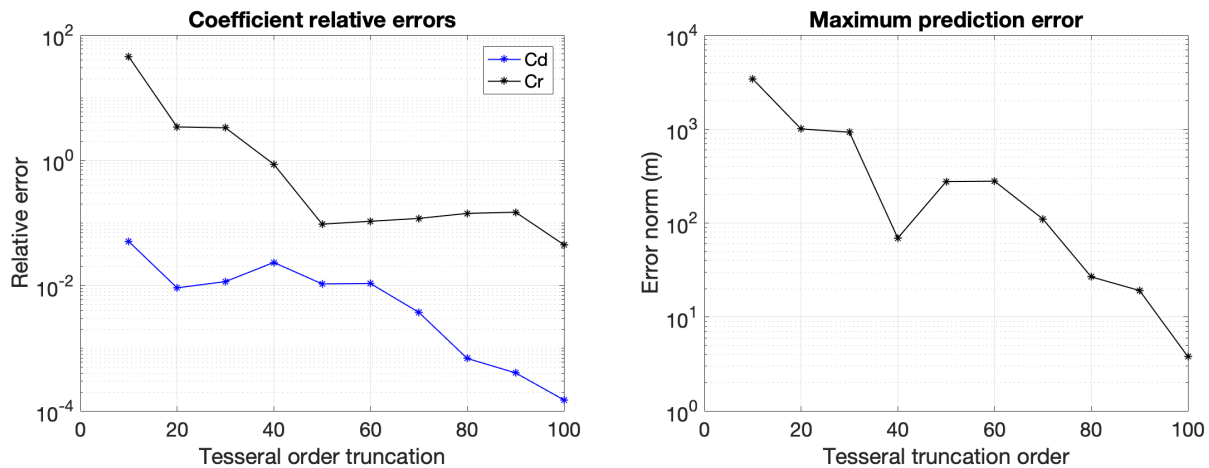
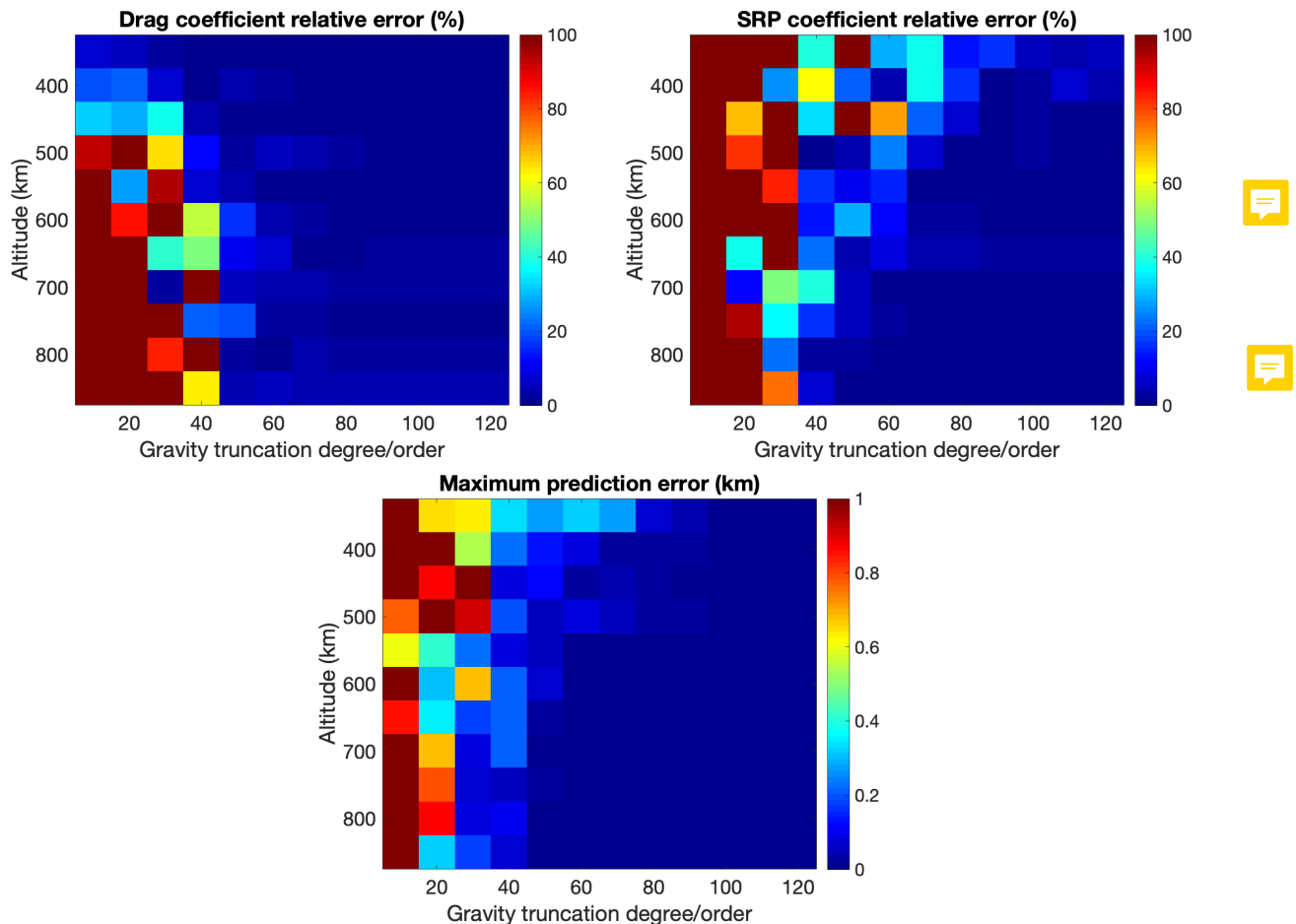


Fig. 9 Relative error in the estimated coefficients (left) and maximum error in the predicted orbits at the end of three days (right) at 350 km with all the zonal terms included

## VII. COEFFICIENT ERROR MAPS

In this section, the relative errors in drag and SRP coefficients are mapped out across the low altitude LEO regime. In section IV, it was observed that in order to obtain a certain accuracy in the coefficient estimates, the required gravity truncation order/degree is dependent on the satellite altitude. In order to select a truncation order/degree for an orbital regime, it is essential to know how much error is introduced into the coefficients at that particular altitude. Therefore, the drag and radiation coefficients are estimated in the altitude range of 350-850 km at every 50 km with truncated gravity models. It should be noted that the drag coefficient increases with altitude while the SRP coefficient remains the same. The coefficient relative error percentages along with the maximum error in the predicted states at the end of three days are plotted in Fig. 10. The coefficient errors are capped at 100 % and the prediction error is capped at 1 km. From the drag coefficient error plot, it can be seen that higher truncation orders are needed in order to obtain a small relative error at higher altitudes and the error seems to be quite small for lower altitudes. But as pointed out in section 3, at lower altitudes, the orbit propagation is very sensitive to errors in the drag coefficient. Therefore, the truncation order will be higher in the lower altitudes as can be seen in the maximum prediction error trend. For example, a truncation order of 100 at 350 km would yield an error magnitude similar to that obtained by a truncation order of 50 at 850 km. As seen in the previous section, even though the coefficient errors are sensitive to changes in factors such as solar activity and area-to-mass ratio, the effective contribution to the orbit propagation remains the same. Therefore, these maps can be referenced for selecting gravity truncation order/degree across the low LEO altitude regime.



**Fig. 10** Clockwise from left: Relative error percentage in the estimated drag coefficient, relative error percentage in the estimated SRP coefficient and maximum error in the predicted orbits at the end of three days. The coefficient error maps are capped at 100 % and the maximum prediction error is capped at 1 km

## VIII. CONCLUSIONS

In this study, we analyzed the correlations between the higher order gravitational forces and the dominant non-conservative forces in the low altitude LEO regime, i.e. atmospheric drag and SRP. Our contention with the current method of gravity field truncation is that simply looking at the contribution of the higher order harmonics towards orbit propagation is not sufficient. The unmodeled gravitational harmonics alias into the free parameters being estimated in the filter, i.e. the drag and SRP coefficients, due to the presence of ignored gravity components along the drag and SRP directions. This leads to higher prediction errors than expected simply from contribution of unmodeled gravity towards orbit propagation. We show that even though the average higher order gravity accelerations can be small compared to drag and SRP, the instantaneous accelerations are comparable to much higher orders. The relative errors introduced into the coefficients closely follow the trend of the ratio of projected unmodeled gravity and non-conservative force. The relative significance of the errors in the drag and SRP coefficients is analyzed for the low LEO altitude regime. At lower altitudes, even though the apparent error in the drag coefficient might be smaller than the SRP coefficient, the effective contribution towards orbit propagation is much higher. The sensitivity of aliasing effects to factors such as orbital parameters, solar activity level and area-to-mass ratios is studied. Decrease in the area-to-mass ratios or solar activity level increases the relative error introduced in the coefficients, but the contribution towards the orbit prediction error remains the same. Therefore, for orbit determination and prediction, these factors can be safely ignored while selecting the gravity truncation degree/order, though they can be important for applications such as atmospheric density derivation. The advantages of using a non-square gravity field have been suggested in literature for orbit propagation. However, when drag and SRP coefficients are being estimated, we find no significant benefits of including more zonal terms than tesseral terms for lowering the estimation errors in the coefficients. Finally, relative error maps for the drag and SRP coefficients are presented to serve as a reference while selecting gravity truncation degree/order in the low altitude LEO regime.

## References

- [1] Lucchesi, D., "Reassessment of the Error Modelling of Nongravitational Perturbations on LAGEOS II and Their Impact in the Lense-Thirring Determination. Part I," *Planetary and Space Science*, Vol. 49, 2001, pp. 447–463. doi:10.1016/S0032-0633(00)00168-9.
- [2] McMahon, J. W., and Scheeres, D. J., "Improving Space Object Catalog Maintenance Through Advances in Solar Radiation Pressure Modelling," *Journal of Guidance, Control, and Dynamics*, Vol. 38, No. 8, 2015, pp. 1366–1381. doi:10.2514/1.G000666.
- [3] Sutton, E. K., "Normalized Force Coefficients of Satellites with Elongated Shapes," *Journal of Spacecraft and Rockets*, Vol. 46, No. 1, 2009, pp. 112–116. doi:10.2514/1.40940.
- [4] Pilinski, A. B. M., Marcin D., and Palo, S. E., "Semi-Empirical Satellite Accommodation Model for Spherical and Randomly Tumbling Objects," *Journal of Spacecraft and Rockets*, Vol. 50, No. 3, 2013, pp. 556–571. doi:10.2514/1.A32348.
- [5] Mehta, P. M., Walker, A., Lawrence, E., Linares, R., Higdon, D., and Koller, J., "Modeling satellite drag coefficients with response surfaces," *Advances in space research*, Vol. 54, 2014, pp. 1590–1607. URL <http://dx.doi.org/10.1016/j.asr.2014.06.033>.
- [6] Ray, V., Scheeres, D. J., Hesar, S. G., and Duncan, M., "Improved drag coefficient modeling with spatial and temporal Fourier coefficient expansions: theory and application," *Advanced Maui Optical and Space Surveillance Technologies Conference (AMOS)*, 2018, pp. 446–461. URL <https://amostech.com/TechnicalPapers/2018/AstroDynamics/Ray.pdf>.
- [7] Montenbruck, O., and Gill, E., *Satellite Orbits: Models, Methods and Applications*, Springer, 2000. doi:10.1007/978-3-642-58351-3.
- [8] Vallado, D., "An analysis of state vector propagation using different flight dynamics programs," *Advances in the Astronautical Sciences*, Vol. 121, 2005. Proceedings of the 15th AAS/AIAA Space Flight Mechanics Meeting, Copper Mountain, CO, January 23–27 2005.
- [9] Barker, W., Casali, W., and Wallner, R., "Earth gravitational error budget for space control," *Advances in the Astronautical Sciences*, Vol. 93, 1996, pp. 351–370. Proceedings of AAS/AIAA Spaceflight Mechanics Meeting, Austing, TX, February 12–15, 1996.

- [10] Roscoe, C. W. T., Griesbach, J. D., Westphal, J. J., Hawes, D. R., and Carrico Jr., J. P., “Force Modeling and State Propagation for Navigation and Maneuver Planning for CubeSat Rendezvous, Proximity Operations, and Docking,” *Advanced Maui Optical and Space Surveillance Technologies (AMOS) Conference*, Wailea, Maui, Hawaii, 2013.
- [11] National Research Council, *Continuing Kepler’s Quest: Assessing Air Force Space Command’s Astrodynamics Standards*, The National Academies Press, Washington D.C., 2012. URL <https://doi.org/10.17226/13456>.
- [12] Pavlis, N. K., Holmes, S. A., Kenyon, S. C., and Factor, J. K., “The development and evaluation of the Earth Gravitational Model 2008 (EGM2008),” *Journal of geophysical research*, 2012. URL <https://doi.org/10.1029/2011JB008916>.
- [13] Picone, J., Hedin, A., Drob, D., and A.C., A., “NRLMSISE-00 Empirical Model of the Atmosphere: Statistical Comparisons and Scientific Issues,” *Journal of Geophysical Research*, Vol. 107, No. A12, 2002, pp. 2035–2051. doi:10.1029/2002JA009430.
- [14] Folkner, W. M., Williams, J. G., Boggs, D. H., Parks, R. S., and Kuchynka, P., “The Planetary and Lunar Ephemerides DE430 and DE431,” IPN progress report, Jet Propulsion Laboratory, February 2014.
- [15] Ray, V., Scheeres, D. J., Hesar, S. G., and Duncan, M., “High-fidelity drag coefficient modeling with spatial and temporal Fourier expansions for orbit determination,” *Journal of astronautical sciences* (2019, under review), ???
- [16] Wang, Y., Lean, J., and Sheeley Jr, N., “Modeling the Sun’s magnetic field and irradiance since 1713,” *The astrophysical journal*, Vol. 625, No. 1, 2005, pp. 522–538.